

# Missense Mutation in Sterile $\alpha$ Motif of Novel Protein SamCystin is Associated with Polycystic Kidney Disease in (*cy/+*) Rat

Joanna H. Brown,\* Marie-Thérèse Bihoreau,\* Sigrid Hoffmann,<sup>†</sup> Bettina Kränzlin,<sup>†</sup> Iulia Tychinskaya,<sup>†</sup> Nicholas Obermüller,<sup>‡</sup> Dirk Podlich,<sup>†</sup> Suzanne N. Boehn,<sup>†</sup> Pamela J. Kaisaki,\* Natalia Megel,<sup>†</sup> Patrick Danoy,<sup>§</sup> Richard R. Copley,\* John Broxholme,\* Ralph Witzgall,<sup>||</sup> Mark Lathrop,<sup>§</sup> Norbert Gretz,<sup>†</sup> and Dominique Gauguier\*

\*The Wellcome Trust Centre for Human Genetics, University of Oxford, Oxford, United Kingdom; <sup>†</sup>Medical Research Centre, Klinikum Mannheim, University of Heidelberg, Mannheim, Germany; <sup>‡</sup>Division of Nephrology, Medical Clinic III, University of Frankfurt, Frankfurt, Germany; <sup>§</sup>Centre National de Génotypage, Evry, France; and <sup>||</sup>Institute for Molecular and Cellular Anatomy, University of Regensburg, Regensburg, Germany

Autosomal dominant polycystic kidney disease (PKD) is the most common genetic disease that leads to kidney failure in humans. In addition to the known causative genes *PKD1* and *PKD2*, there are mutations that result in cystic changes in the kidney, such as nephronophthisis, autosomal recessive polycystic kidney disease, or medullary cystic kidney disease. Recent efforts to improve the understanding of renal cystogenesis have been greatly enhanced by studies in rodent models of PKD. Genetic studies in the (*cy/+*) rat showed that PKD spontaneously develops as a consequence of a mutation in a gene different from the rat orthologs of *PKD1* and *PKD2* or other genes that are known to be involved in human cystic kidney diseases. This article reports the positional cloning and mutation analysis of the rat PKD gene, which revealed a C to T transition that replaces an arginine by a tryptophan at amino acid 823 in the protein sequence. It was determined that *Pkdr1* is specifically expressed in renal proximal tubules and encodes a novel protein, SamCystin, that contains ankyrin repeats and a sterile  $\alpha$  motif. The characterization of this protein, which does not share structural homologies with known polycystins, may give new insights into the pathophysiology of renal cyst development in patients.

*J Am Soc Nephrol* 16: 3517–3526, 2005. doi: 10.1681/ASN.2005060601

**A**utosomal dominant polycystic kidney disease (ADPKD) is one of the most common genetic diseases in humans, affecting all ethnic groups with a prevalence of 1 in 500 to 1000 individuals. The disease is characterized by the progressive formation and enlargement of fluid-filled cysts in both kidneys that leads to renal failure. In the diseased kidney, epithelial cysts are present in all parts of the nephron. Cyst development involves impairments in a wide range of cellular processes, including increased proliferation of the renal epithelial cells, fluid transport defects, alterations in tubular basement membrane, altered cell polarity, and increased apoptosis (1).

Two genes that are responsible for ADPKD, *PKD1* and *PKD2*, which encode polycystins, have already been characterized in humans. Mutations in these proteins account for the vast majority of ADPKD cases (1). However, a small number of families

with ADPKD have been reported to develop PKD that seems to be unlinked to either *PKD1* or *PKD2*, leading to the controversial suggestion of the involvement of other as-yet-unknown genes (1,2). Furthermore, several other, although less frequent, hereditary cystic kidney diseases that also lead to terminal renal failure (1) occur in childhood, adolescence, or adulthood (e.g., autosomal recessive polycystic kidney disease, nephronophthisis, medullary cystic kidney disease).

Rodent models of spontaneous renal cyst disorders are powerful systems to characterize the pathophysiologic mechanisms involved and potentially point to new candidate genes that contribute to human cystic diseases (3). Of the available rat models, altered physiologic and morphologic renal phenotypes of the inbred (*cy/+*) rat strain closely resemble human ADPKD (4,5). Renal cyst lesions progressively develop from the first few weeks of life, and gender differences in disease severity have been reported. In addition, this model is characterized by a slow progression of uremia, proteinuria, and hyperlipidemia. In three independent genetic studies, the gene that is responsible for PKD in (*cy/+*) rats has been localized to a large, poorly defined region on rat chromosome 5 (6–8) spanning between 15 and 5 cM according to the different published linkage maps (9,10). This locus, which is denoted *Pkdr1*, does not share homology relationships with the gene loci *PKD1* or *PKD2* (6).

Received June 8, 2005. Accepted August 13, 2005.

Published online ahead of print. Publication date available at [www.jasn.org](http://www.jasn.org).

J.H.B. and M.-T.B. contributed equally to this work.

**Address correspondence to:** Dr. Marie-Thérèse Bihoreau, The Wellcome Trust Centre for Human Genetics, University of Oxford, Oxford OX3 7BN, UK. Phone: +44-01-865-287-648; Fax: +44-01-865-287-533; E-mail: [bihoreau@well.ox.ac.uk](mailto:bihoreau@well.ox.ac.uk)

To identify the PKD susceptibility gene in the (*cy/+*) rat, we combined traditional physical and genetic mapping methods with computational analyses of the emerging sequence of the rat genome at the refined *Pkdr1* locus. We report that the susceptibility gene encodes a novel protein, SamCystin, which contains both ankyrin repeats and a sterile  $\alpha$  motif (SAM), in which we identified a missense mutation in the PKD affected rat strain. This protein, strongly expressed in kidneys, does not share structural similarities with known polycystins or other proteins that are known to be involved in cystic kidney diseases. Our findings provide new perspectives to elucidate the pathophysiology and genetic causes of cystic kidney disorders in human patients.

## Materials and Methods

### *Animals and Phenotype Analysis*

The colony of inbred PKD/Mhm(*cy/+*) rats [formerly called Han:SPRD(*cy/+*)] used in this study was established in our laboratory in Mannheim after 18 additional generations of inbreeding of the Han:SPRD(*cy/+*) rat strain obtained from Dr. Deerberg (Central Institute for Laboratory Animal Breeding, Hanover, Germany; <http://www.informatics.jax.org/external/festing/rat/docs/PKD.shtml>). Brown Norway (BN) rats were obtained from Elevage Janvier (St. Ille, France).

A large cohort of 742 first-backcross (BC1) rats was derived from affected F1(*cy/+*) rats that were mated to BN rats as described previously (11). The BN rat was preferred to other inbred rat strains because of the high level of allele variation observed between BN and PKD/Mhm(*cy/+*) strains, which facilitates the detection of recombinant hybrids in the BC1 cohort and therefore increases efficiency of positional cloning the disease gene. All hybrids were killed at day 36. Kidneys were removed, weighed, fixed in 3% buffered formaldehyde, and then embedded in paraffin for histologic analyses. After hematoxylin/eosin staining of kidney sections, presence of renal cysts was assessed by microscopic examination (11).

### *Microsatellite and Gene Markers*

All available markers that are known to map in the vicinity of the locus *Pkdr1* were selected from public rat genetic databases ([http://www.well.ox.ac.uk/rat\\_mapping\\_resources](http://www.well.ox.ac.uk/rat_mapping_resources); <http://rgd.mcw.edu>) and tested for allele variation between the PKD/Mhm(*cy/+*) and BN rat strains. A total of 22 markers that already are genetically mapped (9,10) and/or localized on the T55 rat radiation hybrid panel (9,12) were selected to initiate this study.

We used data from existing comparative maps between rat chromosome 5 and mouse and/or human chromosomes (10,12) to search human (<http://www.ncbi.nlm.nih.gov>) and mouse (<http://www.informatics.jax.org>) public genome databases to establish a gene map of the original *Pkdr1* locus (6), which was designed to facilitate physical mapping of the locus. Rat gene sequences that are homologous to human and mouse genes that were predicted to map at the *Pkdr1* locus were identified by BLAST query. A list of human orthologous genes that mapped to the *Pkdr1* interval was established using both the Human Genome Browser (<http://genome.ucsc.edu>) and Ensembl (<http://www.ensembl.org>). Rat sequences (mRNA and expressed sequence tag [EST]) homologous to each human sequence were accessed, when possible, *via* the data mining tools provided by the National Center for Biotechnology Information (<http://www.ncbi.nlm.nih.gov>). Rat sequences were also identified through other public rat genome databases, the Ulowa Rat EST Project (<http://ratest.uiowa.edu>) and RAT-MAP (<http://ratmap.gen.gu.se>). Since 2003, the release of the rat genome

sequence ([http://www.ensembl.org/Rattus\\_norvegicus](http://www.ensembl.org/Rattus_norvegicus); <http://genome.ucsc.edu>) has accelerated rat gene annotation and comparative genome analysis (10) and increased the number of new informative microsatellite markers for the positional cloning of *Pkdr1*.

Oligonucleotides for new rat microsatellites were designed using the OLIGO 4.0 computer program (National Biosciences Inc., Plymouth, MN). PCR primer pairs were synthesized commercially by Sigma Genosys (Pampisford, UK).

### *Genotype Determination*

Microsatellite markers that showed evidence of allele variation between the PKD/Mhm(*cy/+*) and BN strains were typed on either the complete BC1 cohort or, after progress in the positional cloning of *Pkdr1*, a selection of recombinant hybrids. PCR amplification and genotyping procedures were carried out as described previously (6).

### *Physical Mapping and Sequence Tagged Site Screening*

Both rat microsatellites and gene/EST markers that mapped to the original *Pkdr1* locus were used for screening rat yeast artificial chromosome (YAC), bacterial artificial chromosome (BAC), and P1-derived artificial chromosome (PAC) libraries. Standard PCR screening methods were used to isolate YAC clones from the rat LPY library (<https://www.resgen.com>). YAC ends were obtained by use of vectorette bubble PCR (13) and sequenced directly using the BigDye Terminator kit (Perkin-Elmer/Applied Biosystems, Warrington, UK) to generate new markers and allow chromosome walking. Rat BAC clones were isolated from the RPCI-32 library (<http://bacpac.chori.org>) and PAC clones from the RPCI-31 library (14) by hybridization of radioactively labeled probes to high-density gridded nylon filters as described previously (14). BAC/PAC end sequences from strategically selected BAC and PAC clones were obtained using the same method as for YAC ends. Sequence tagged site content maps were assembled by PCR amplification of DNA miniprepations from the isolated clones.

### *RNA Isolation and cDNA Preparation*

Total RNA was extracted from whole kidneys of 2-wk-old PKD/Mhm(*cy/cy*), PKD/Mhm(*cy/+*), PKD/Mhm(+/+), BN, and Lewis rat strains using the TRIZOL reagent (Life Sciences, Paisley, UK), followed by a clean-up with the RNeasy kit (Qiagen, Crawley, UK). First-strand cDNA was synthesized from 5  $\mu$ g of total RNA using Superscript II RNase HReverse Transcriptase (Invitrogen, Paisley, UK).

### *Sequencing and In Silico Sequence Analysis*

Cycle sequencing was carried out using BigDye terminators (Perkin-Elmer/Applied Biosystems), followed by either ethanol precipitation or Sephadex G50 filter plate purification, and sequences were run on ABI 377 or 3700 automated sequencers. cDNA were sequenced in both directions using PCR primer pairs that amplified overlapping cDNA fragments designed along the full-length coding sequence. Raw sequence data were analyzed and assembled using the University of Washington's suite of programs PHRED, PHRAP, and CONSED ([www.phrap.org](http://www.phrap.org)). For clone sequencing, vector and repeat sequences were masked and high-quality sequence was compared with available sequence databases using an in-house search program. The AceDB genome database program was used to display and manage this information (<http://www.acedb.org>). Mutation screening was performed on 20 different inbred rat strains and substrains, including BN, Lewis, GK, SHR, SHRSP, WKY, BB, GAERS, DA, ACI, Wistar-Furth, Zucker, and Fisher.

### PCR-RFLP Analysis

The R823W C/T mutation was detected using PCR-RFLP. PCR with primers (CTAGAAGCCTCAGTGACCCC, CAGCGTGTGAACAAGG-TAGG) designed from corresponding genomic DNA sequence was carried out as described previously (6). PCR products of length 242 bp were digested with *Msp I* restriction endonuclease (Boehringer Mannheim, Mannheim, Germany) that recognizes and cuts the wild-type (into two fragments of 157 and 85 bp) but not the mutated sequence site of PCR products. Reactions were incubated at 37°C for 1 h. The digested PCR products were resolved on an agarose gel.

### Gene Transcription Analysis

A commercial panel of cDNA that was prepared from multiple rat tissues (Rat MTC Panel I; Clontech, Oxford, UK) was used to test the expression of the *Pkdr1* gene in eight different tissues. We designed the WC4 primer pair (CTTCGAGCCAAAAACGGAT, CAGCATGGTCGT-CAGTAACAC) to amplify a 462-bp cDNA segment between the ankyrin (ANK) and SAM domains of *Pkdr1* to ensure maximum specificity. Transcript levels for the B2 microglobulin housekeeping gene served as a cDNA loading control.

Northern blots were performed with 20 µg of total RNA that was prepared from kidneys of 21-d-old PKD/Mhm(*cy/cy*), PKD/Mhm(*cy/+*), and PKD/Mhm(+ / +) rats. RNA was size-fractionated on a 0.8% formaldehyde-agarose gel and transferred to nylon membranes (Hybond N; Amersham, Braunschweig, Germany). A <sup>32</sup>P random primer-labeled 1.6-kb fragment of *Pkdr1* cDNA was prepared as gene-specific probe. Hybridization was carried out with a 50-mM sodium phosphate buffer (pH 7.0) that contained 50% formamide, 5× SSC, 5× Denhardt's solution, 1% SDS, and 250 µg/ml denatured salmon sperm DNA, followed by washes in SSC/SDS solutions. Detection of the rat glyceraldehyde-3-phosphate dehydrogenase mRNA levels was used as loading standard. Transcripts were visualized on a FUJI BAS 2500 PhosphorImager (FUJI, Dusseldorf, Germany).

### In Situ Hybridization

For kidney *in situ* hybridization, rats were killed by retrograde perfusion through the distal abdominal aorta with 0.9% sodium chloride for 3 min at pressure level of 220 mmHg. Kidney slices were immersed in 4% paraformaldehyde in PBS for 2 to 4 h, then in 18% sucrose for 2 h before being slowly frozen in isopentane at -30°C and placed directly into liquid nitrogen. Five- to 7-µm cryosections were postfixed in 4% paraformaldehyde in PBS, acetylated in 0.1 M triethanolamine (pH 8.0) that contained 0.25% acetic anhydride. The slides were dehydrated in graded ethanol up to 95% and air-dried. Sense and antisense *Pkdr1* cRNA probes spanning the whole cDNA were generated by *in vitro* transcription using digoxigenin-11-UTP (Roche, Mannheim, Germany) according to the manufacturer's instructions. Transcripts were subjected to partial alkaline hydrolysis to improve penetration. *In situ* hybridization was carried out as described previously (15). Briefly, sections were hybridized with a solution that contained 50% formamide and 5 to 8 ng/µl RNA probe overnight at 48°C and stringently washed. Sections then were incubated with a polyclonal alkaline phosphatase-coupled sheep anti-digoxigenin antibody. Signal detection was performed with NBT/X-phosphate, and the color reaction was controlled under the microscope. Sense probes did not produce any detectable signal. On consecutive cryosections, postfixed in 4% paraformaldehyde in PBS, staining for endogenous alkaline phosphatase was performed using NBT/X-phosphate as a substrate.

### Western Blot Analysis

cDNA were subcloned into the eukaryotic expression vector pEBG, which encodes fusion proteins with glutathione S-transferase at their

NH<sub>2</sub>-terminus. COS-7 cells were transiently transfected using the DEAE-dextran method (16). Cells were lysed in 1× PBS/1% Triton X-100, and the protein concentration was determined using an improved Bradford assay (17). Equal amounts of protein were separated under reducing conditions on a denaturing SDS-polyacrylamide gel, transferred onto a polyvinylidene difluoride membrane, and then incubated with a mouse monoclonal anti-GST antibody (diluted 1:3000; Sigma, St. Louis, MO) as primary antibody. Specifically bound primary antibody was detected with a horseradish peroxidase-conjugated goat anti-mouse secondary antibody and subsequent chemiluminescence.

## Results

### Construction of the Physical Map

Neither rat physical maps nor rat genome sequence data were available when we carried out the positional cloning of the *Pkdr1* gene. We initiated the construction of a physical map of the *Pkdr1* locus using 32 published microsatellite markers that were obtained from repositories of rat genetic and genomic resources. We assembled a scaffold of rat YAC contigs spanning the 37 Mb (approximately 15 cM [18]) of the *Pkdr1* locus between D5Rat2 and D5Mgh6. These contigs covered all PKD quantitative trait loci reported on chromosome 5 in crosses derived from (*cy/+*) rat (6–8). The initial YAC physical map was enriched by a chromosome walking strategy, with end markers checked for chromosomal location on the rat T55 radiation hybrid panel (12). Chromosomal mapping of a selection of clone inserts was verified by fluorescence *in situ* hybridization (data not shown). This map was converted into a more useful high-resolution form by isolating BAC and PAC clones, which were anchored to the YAC framework by virtue of their sequence tagged site content. Using these methods, we identified a total of 108 YAC and 44 BAC/PAC clones across the *Pkdr1* region and assembled three major clone contigs. A simplified overview of the physical map is shown in Figure 1b. A full description of the physical map is available through our rat database ([http://www.well.ox.ac.uk/rat\\_mapping\\_resources](http://www.well.ox.ac.uk/rat_mapping_resources); supplemental material available online: Annex 1). After comparative genome analysis between human, mouse, and rat, 23 new rat gene markers were localized in the physical map by PCR amplification of DNA from YAC, PAC, or BAC assigned to the contigs.

### Fine Genetic Mapping of *Pkdr1* Locus

In parallel with chromosome walking, we constructed a high-resolution genetic map of the region of interest and identified, among the 742 BC1 [PKD/Mhm(*cy/+*)xBN], animals that carry recombinations within the *Pkdr1* locus. Ninety-seven new microsatellite markers were produced by clone-end sequencing as well as shotgun sequencing of inserts from selected BAC and PAC clones that were isolated from the physical map. Fourteen BAC and PAC clones were partially shotgun sequenced (unpublished data), from which 75 microsatellite markers were generated, 31 of which were polymorphic between PKD/Mhm(*cy/+*) and BN strains and could be tested on the recombinant panel. Integrating new markers in the clone contigs allowed their physical order to be resolved. Marker information is available through our database ([http://www.well.ox.ac.uk/rat\\_mapping\\_resources](http://www.well.ox.ac.uk/rat_mapping_resources)).

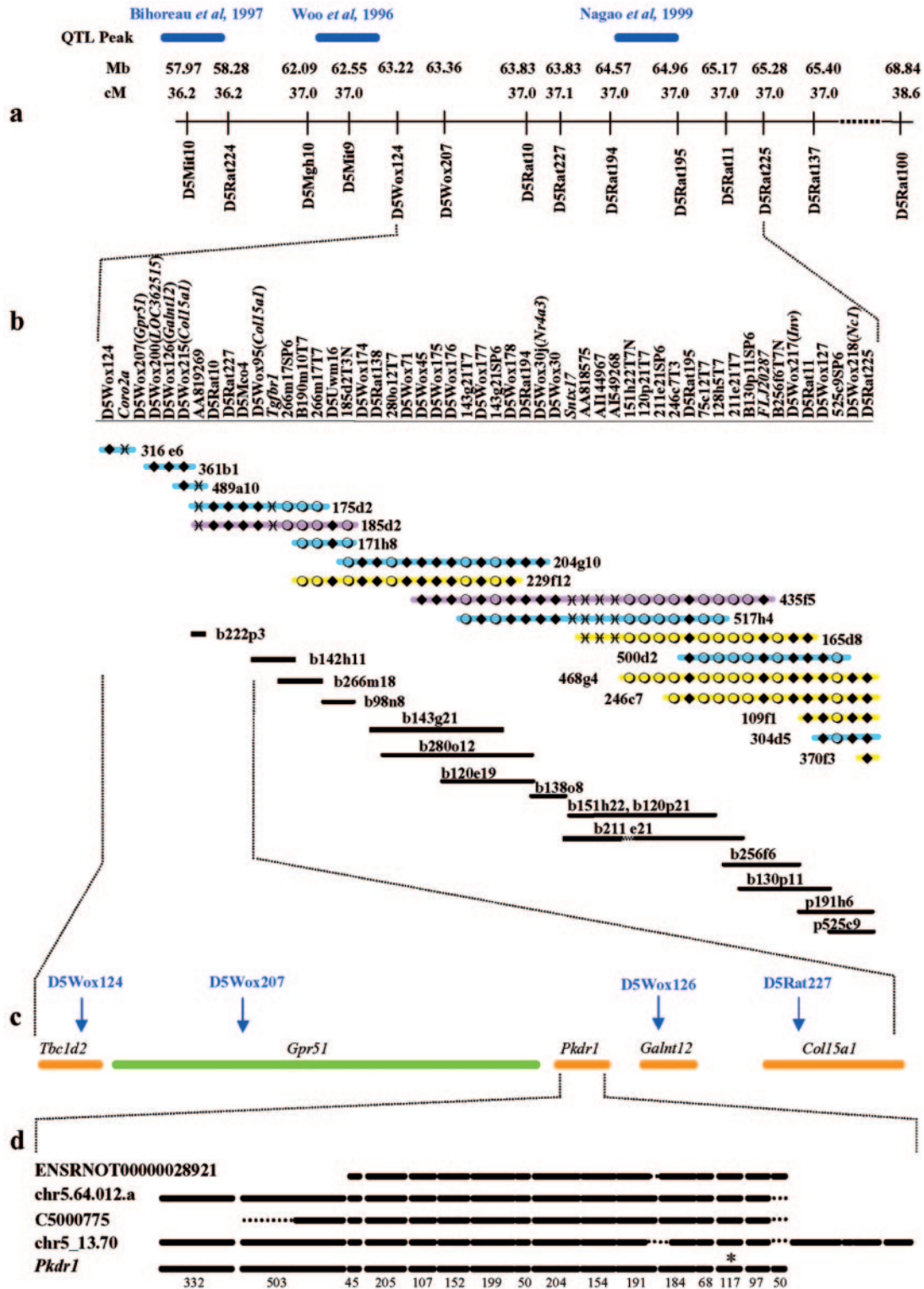


Figure 1. The *Pkdr1* locus and transcript. (a) Chromosome 5 genetic map (cM) and position of the peaks of previously reported polycystic kidney disease (PKD) quantitative trait loci (QTL) in the *cy* rat (6–8). Physical positions (Mb) are according to the UCSC Genome Browser (June 2003 build). Distances between markers are not to scale. (b) Physical map for a portion of the *Pkdr1* locus. Yeast artificial chromosome clones are purple if nonchimeric, yellow if chimeric, and blue if their chimera status is unknown. Markers are represented by  $\blacklozenge$  if microsatellites, by  $\circ$  if clone ends, and by  $\ni$  if expressed sequence tag. Bacterial artificial chromosome and P1-derived artificial chromosome shown beneath are denoted by solid black lines. (c) Annotation of the chromosomal interval defined by recombinant mapping for known and predicted genes (in green and orange, respectively). (d) Genomic structure of four *Pkdr1* gene predictions and the final version derived from cDNA sequencing. Solid black lines represent the exons, and numbers indicate exon length (bp). In *Pkdr1*, the asterisk shows the location of the C→T missense mutation.

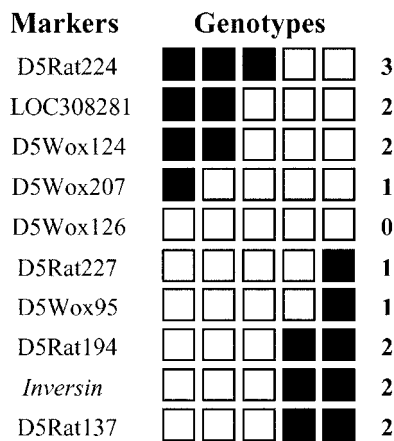


Figure 2. Genetic mapping of the *Pkdr1* locus between D5Rat224 and D5Rat137. ■, recombinant genotype at the marker; □, no recombination. The values to the right are the numbers of recombinant progeny for each marker.

The primary genetic screening of the BC1 cohort identified 45 hybrids that show recombinations within the locus *Pkdr1*. Subsequent extensive genotyping of these 45 rats led to the refinement of the disease locus to a critical region of approximately 1 cM between D5Rat224 and D5Rat137 (Figures 1 and 2). It also allowed the exclusion of some potential PKD candidate loci, such as *Inv*, *Sntx17*, *Grhpr*, and *Tmeff1*, which were identified by comparative genome analysis of the *Pkdr1* locus. The BC1 rat panel was finally reduced to five recombinant animals that were genotyped with additional microsatellite markers generated from the emerging rat draft genomic sequence covering the region of interest ([http://www.ensembl.org/Rattus\\_norvegicus](http://www.ensembl.org/Rattus_norvegicus); <http://genome.ucsc.edu>). Strong PKD candidate genes then could be excluded (LOC308281 similar to dynactin *DCTN3*, a dynein re-

lated to *DNAI1*, *Cntr*, *Tbc1d2*, *Gpr51*, and *Col15a1*). The critical interval was eventually reduced to 0.47 Mb between D5Wox207 and D5Rat227, where only two genes (*Galnt12* and a novel gene) have been annotated by *in silico* mapping (Figures 1c and 2). D5Wox126, localized in the genomic sequence of *Galnt12*, was checked in the entire BC1 cohort for absence of any recombinant genotypes.

Sequence Analysis of Positional Candidate Genes

The gene encoding the UDP-N-acetyl- $\alpha$ -D-galactosamine: polypeptide N-acetylgalactosaminyltransferase 12 (*Galnt12*) and an unknown gene (LOC362515), predicted to encode a protein that contained ANK repeats and a SAM domain, were evaluated for sequence mutations in their respective coding sequence. For that purpose, cDNA were prepared from kidneys of PKD/Mhm(*cy*/+), PKD/Mhm(*cy*/*cy*), PKD/Mhm(+/+), BN, and Lewis rats. No sequence variants between the four strains were found in *Galnt12*. Sequence analysis of the cDNA of the novel gene revealed a C→T transition in the *cy* rat that was absent in 20 different inbred rat strains, including the Sprague Dawley strain in which the spontaneous *cy* mutation initially arose (Figure 3a). The mutation was also present in the *cy* rat strain of the American colony (7) derived from the original Han:SPRD(*cy*/+) strain (Figure 3b). By BLAST alignment of our cDNA sequence with rat genomic clone AC132650, we deduced the exonic boundaries and established that the gene contains 16 exons spanning an open reading frame of 2.655 kb (Table 1) encoding a putative protein of 885 amino acids. The intron-exon structure, submitted to GenBank (AY661303), emerged as being slightly different from that predicted by various programs used for gene annotations (Figure 1d). The transcript prediction that was obtained with the TwinScan program omitted exon 16, whereas gene annotation by the Ensembl automatic analysis pipeline skipped exons 1 and 2 and

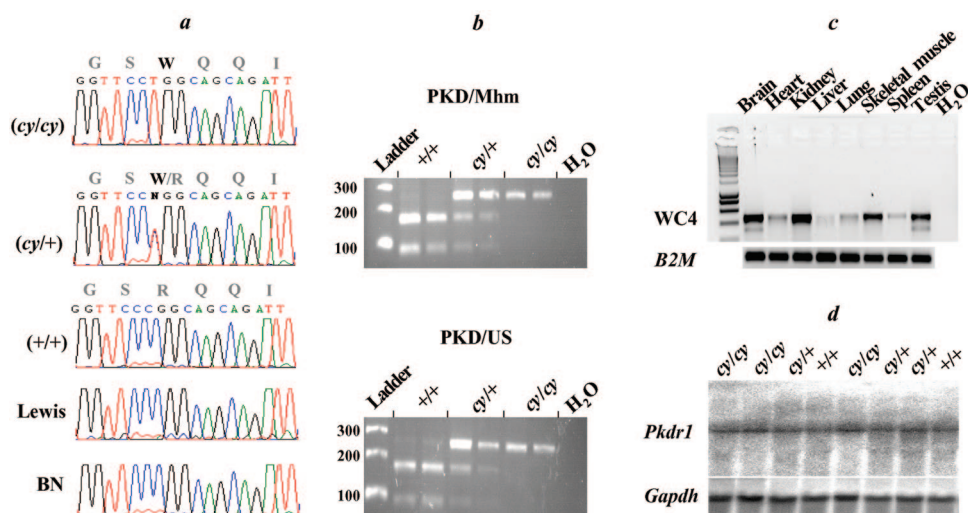


Figure 3. Expression and sequence analysis of *Pkdr1*. (a) Sequence traces of cDNA from PKD/Mhm (*cy*/*cy*), PKD/Mhm(*cy*/+), PKD/Mhm(+/+), BN, and Lewis rat strains showing the C→T transition mutation. The PKD/Mhm(*cy*/+) rat displays a heterozygous genotype at this nucleotide. (b) Detection of the R823W mutation detection by PCR-RFLP analysis in *cy* rats of the PKD/Mhm and American (PKD/US) colonies. (c) Reverse transcription-PCR analysis of the *Pkdr1* transcript in rat tissues using the WC4 marker. (d) Northern blot of total kidney RNA from PKD/Mhm(*cy*/*cy*), PKD/Mhm(*cy*/+), and PKD/Mhm(+/+) rats.

Table 1. Exon–intron boundaries of the *Pkdr1* gene

Exon	Exon Size (bp)	Acceptor Site	Donor Site	Intron	Intron Size (bp)
1	332		GCGGCCAGgtgagcgg	1	6898
2	503	tccggcagGTGTGGGC	GAAAACAGgtcagacc	2	2933
3	45	ttaccagATGAGGAG	GAAGATGGgtaagtgc	3	970
4	205	gtttgcagGAACTTC	TACCATGGgtctgtgt	4	1137
5	107	ctccccagAAATAAAG	TGATCCTGgtgagtca	5	2708
6	152	gccacagACACTGAA	GCCTGAAGgtttgaaa	6	1123
7	199	ccacacagTCCTGGTG	AGACAGTGgtgagaag	7	698
8	50	ttttgcagGCCCTGGG	CGACCATGgtgagtgg	8	2888
9	204	tgtttcagCTGCGCAA	CAGACGGTgtaagtca	9	2739
10	154	actcacagGCTGCTGG	CCGCTCAGgtaagcag	10	2153
11	191	ctcctcagGTGGCAGC	GCAGCAAGgtgcttgt	11	≥3374
12	184	ctgtgcagAAACTGGA	CGATGAGGgtgagtcc	12	1332
13	68	tcatgaagATGAGCTG	AGCAAGAGgtaagaag	13	1842
14	117	ctccccagGTGGACAT	CGGGCAAGgtactgtg	14	5541
15	97	gtccacagGGGCGTGA	CAGTCCCTgtactgta	15	707
16	50	aaccaagCCATGGCC			

altered exon 11. The Fgenesh++ program left out exons 1 and 16 and partially exon 2. Genscan computed a much longer gene with 19 exons but reduced the sequence of exons 11 and 12. The missense point mutation occurs in exon 14 and changes an arginine (CGG) to a tryptophan (TGG) at amino acid 823 within the SAM domain of the new protein, which we named SamCystin.

#### *Pkdr1* Transcription Analysis

The expression of *Pkdr1* in different rat tissues was evaluated in a panel of cDNA by amplifying a gene-specific reverse transcription–PCR product generated by the WC4 marker. The *Pkdr1* transcript was detected with highest abundance in kidney. In common with other PKD genes, it seems to be widely expressed with moderate levels in brain, skeletal muscle, and testis (Figure 3c). By Northern blot analysis, a unique approximately 3.9-kb transcript for *Pkdr1* was detected in kidneys of 21-d-old PKD/Mhm(*cy/cy*), PKD/Mhm(*cy/+*), and PKD/Mhm(+ / +) rats (Figure 3d). *Pkdr1* transcript levels were similar in the three rat groups, suggesting that the mutation affects protein function rather than transcription regulation.

*In situ* hybridization on normal adult rat kidney sections using a *Pkdr1*-specific digoxigenin-labeled antisense riboprobe showed strong mRNA expression in proximal tubules of the cortex and in the outer stripe of the medulla (Figure 4a) but not in the medulla. Higher magnification of the kidney cortex (Figure 4b) showed the specific cytoplasmic localization of labeled *Pkdr1* mRNA in proximal tubules, corresponding to the site of cyst formation in *cy/+* rats. This was confirmed by specific labeling of the proximal tubules using a substrate for alkaline phosphatase (Figure 4, d and e). Similar findings were obtained on kidney sections of PKD/Mhm(*cy/+*) rats (Figure 4, c and f).

#### Conservation of the SamCystin Amino Acid Sequence

Using tblastn searches (<http://www.ncbi.nlm.nih.gov/BLAST>) and the genewise program (<http://www.ebi.ac.uk/>

Wise2), we identified apparent orthologs of rat *Pkdr1* in the genome sequences of mouse, human, *Fugu rubripes* (pufferfish), and *Ciona intestinalis* (a tunicate) (19,20) (Figure 5). The predicted protein sequence of the mouse and human orthologs is shown in the supplemental materials (Annex 2; available online). In all of these species, the arginine residue that is mutated in the rat sequence of the SAM domain is conserved, suggesting that it is functionally important. Among proteins from the genomes of human, *Drosophila* and *Caenorhabditis elegans* that contain a SAM domain C-terminal to ANK repeats, only six of 21 do not have an arginine at this position, and in only two of the six cases, the residue is hydrophobic. Tryptophan is not found in any cases.

#### SamCystin Expression

Protein extracts of COS-7 cells, transiently transfected with the SamCystin expression vector, were analyzed by Western blot with an antibody against glutathione S-transferase (GST). The wild-type and mutant GST-SamCystin fusion proteins migrate to the same position between 83- and 175-kD markers (Figure 6), consistent with their predicted size of 120 kD. COS-7 cells that were transfected with a plasmid that did not encode a fusion protein with GST served as a negative control and did not yield a band.

#### Discussion

We report the positional cloning of a gene encoding a novel protein, SamCystin, which is mutated in the *cy* rat. We have established the correct cDNA and protein sequences of rat SamCystin, highlighting significant differences with all predicted *in silico* annotations of the gene, and determined the expected sequences of the mouse and human orthologs. The implication of SamCystin in renal cyst development derives from the gene expression specific to proximal tubules, the structure of the protein that combines ANK repeats and a SAM

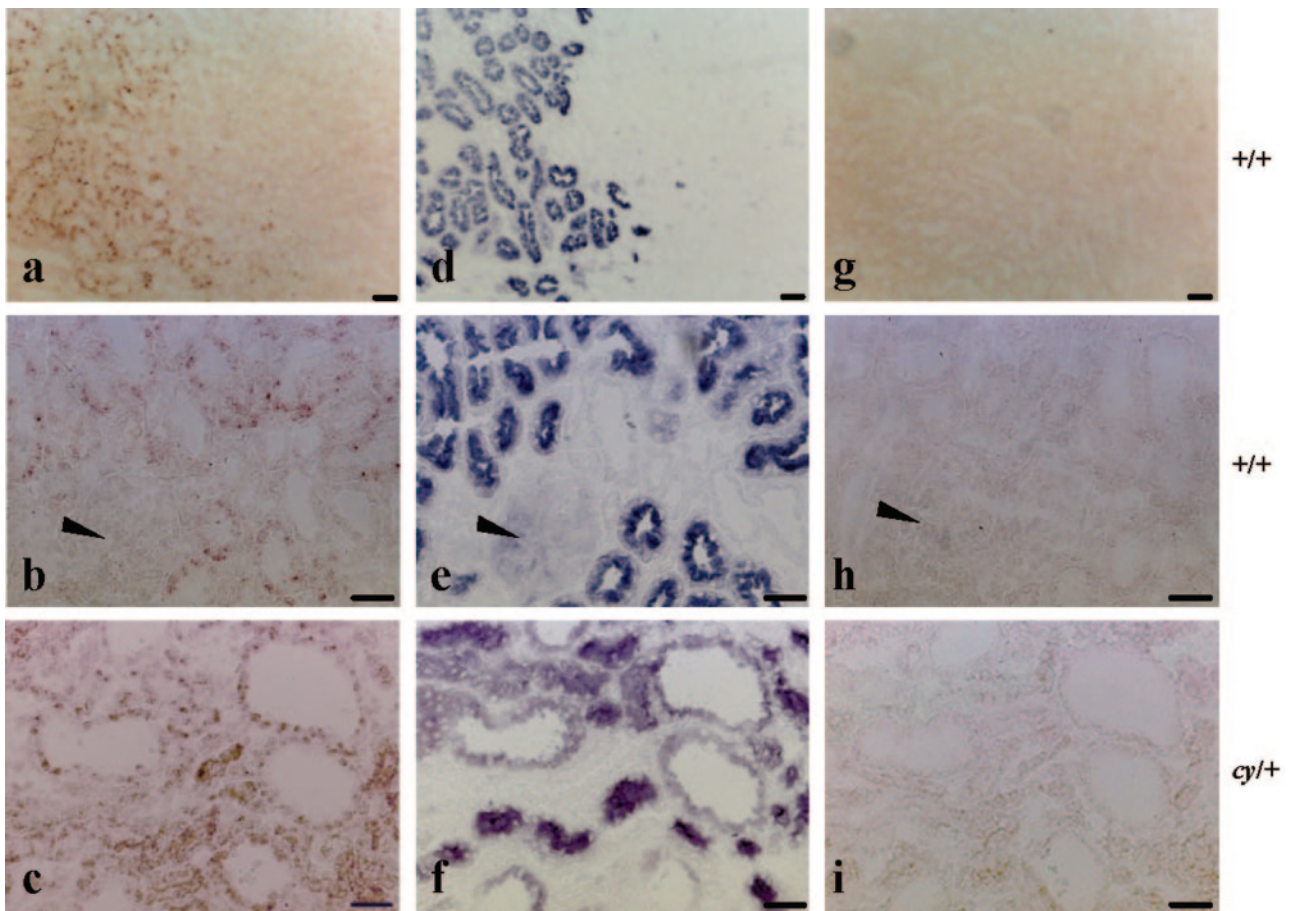


Figure 4. *Pkdr1* expression in the kidney. Overview of normal kidney (top) and higher magnification of normal and cystic kidney cortex (middle and bottom). (a through c) *In situ* hybridization with antisense *Pkdr1* cRNA probe spanning the whole coding sequence showing strong mRNA expression in proximal tubules of the cortex. (d through f) Specific staining of proximal tubular cells with a substrate for alkaline phosphatases. (g through i) Using a sense riboprobe, no specific staining is seen. The arrow indicates a glomerulus. Bar = 40  $\mu$ m.

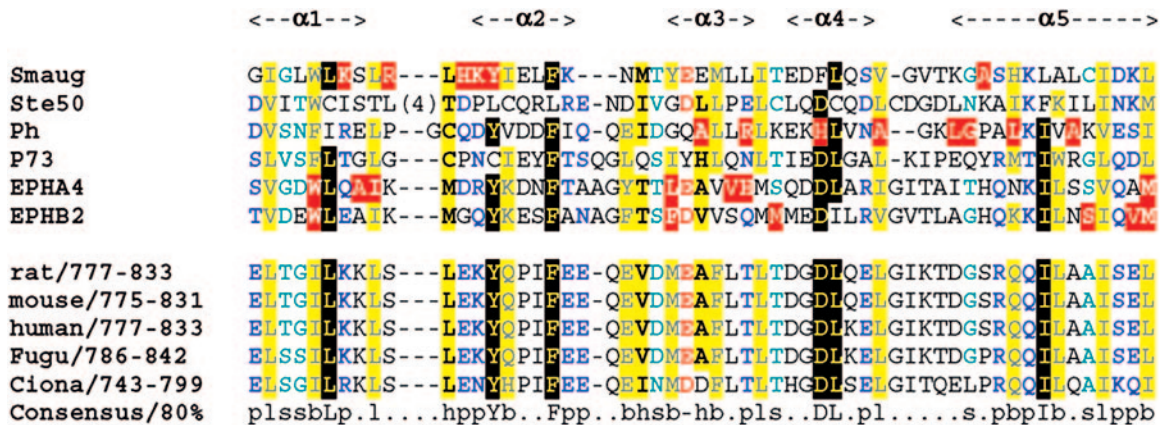
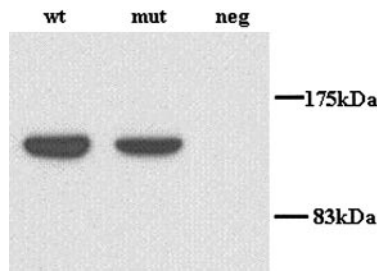


Figure 5. Structure based alignment of sterile  $\alpha$  motif domains, showing equivalent region in vertebrate orthologs of SamCystin. Residues colored in red are involved in homodimer interactions (Ph and EPHA4) or RNA binding (Smaug). Other residues are colored by conservation across the whole alignment as per Chroma defaults (47). Consensus secondary structures are marked above the alignment. The structural alignment was produced using the STAMP package (48). RCSB Protein DataBase (PDB) codes: Smaug 1ojx; Ste50 1uqv; Ph 1kw4; P73 1dxs; EPHA4 1b0x; EPHB2 1b4f. The arrow points out the amino acid mutated in the *cy/+* strain.



**Figure 6.** Detection of wild-type and mutant SamCystin by Western blot analysis. Protein extracts of COS-7 cells transiently transfected with wild-type (wt) and mutant (mut) fusion constructs were analyzed. neg, negative control.

domain, and the position of the R to W missense mutation in the SAM domain of SamCystin in the PKD affected rat strain.

Although the cellular function of SamCystin and the role of the mutation in renal cyst formation in the PKD/Mhm(*cy*/+) rat are unknown, we can anticipate an involvement of SamCystin in protein scaffolding from the presence of two key features: the ANK motifs and the SAM domain. The ANK repeats are tandem repeats of approximately 33 amino acids that are composed of a  $\beta$ -hairpin and two  $\alpha$ -helices that provide a site for protein–protein interaction and are reported to be present in transcription factors and cytoskeleton proteins (21). The SAM domain is a protein–protein and protein–nucleic acid interaction module of approximately 70 amino acids that is found in a variety of proteins, including scaffolding proteins, transcriptional and translational regulators, tyrosine and serine/threonine kinases, and RNA-binding proteins (22–25). As the residues that are implicated in RNA binding in Smaug (26) are not conserved in the SamCystin SAM domain (Figure 5), it seems more likely that it participates in protein–protein interactions. The SAM domain functions in protein interactions as a result of its ability to self-associate (27), bind other SAM domains (28), and form interactions with non-SAM domain-containing proteins (29–32). The precise residues that are responsible for oligomer formation between SAM domains vary considerably depending on the protein (22) (Figure 5). Accordingly, it is not possible to infer directly that the R-W mutation disrupts a protein–protein interaction interface. The low sequence similarity of SamCystin to any SAM domains of known structure (29% at best, to that of Smaug) hampers accurate prediction of the precise local environment of the native arginine side chain. However, its position adjacent to a loop region that is involved in self-association of Ph SAM domains suggests that disruption that is caused by accommodation of the very different biochemical properties of the tryptophan residue may affect the ability of the SamCystin protein to form complexes.

The presence of both SAM and ANK motifs in SamCystin indicates that this novel protein binds simultaneously to multiple interaction partners and self-associates to form large high molecular mass complexes. There are several known proteins that contain a combination of these two motifs together, including SANS (33), the SHANK family (34), CASK-interacting proteins (35), TANK (36), and GASZ (37).

Functional mutations that alter SAM protein domains have already been described in human and mouse models. The SAM domain of the mouse homolog of the *Drosophila* Bicaudal C gene, *Bicc1*, which is expressed in cilia (3) and shares extensive similarities with that of SamCystin, is either altered or truncated in the *jcpk* and *bpk* mouse models of PKD (38). The role of the protein encoded by *Bicc1* in developmental processes in *Drosophila* (39) suggests that it is required for establishing and maintaining normal tubule architecture, with its SAM domain playing a key role (38). Mutations in the SAM domain of the SANS protein have been associated with deafness in human (33) and in the Jackson shaker deaf mutant mouse (40). Disruptions of the hair bundles, which are mechanoreceptive structures of inner ear sensory cells, in these mice suggest that SANS may function as an anchoring/scaffolding protein in cochlea hair cells mediated by protein–protein interactions (40). These results may be particularly relevant to the function of SamCystin in PKD in the PKD/Mhm(*cy*/+) rat because SamCystin and SANS are currently the only known proteins that contain ANK and SAM domains exclusively and recent evidence suggests a causal link between ADPKD and dysfunction in renal ciliary structures (41), which may be the kidney mechanosensory equivalent of the auricular hair bundles.

A direct role of the SAM domain of SamCystin in polycystin-1-related signaling pathways cannot be ruled out. After chromosomal rearrangement, the SAM domain of the TEL (translocation Ets leukemia) transcriptional repressor fuses to a variety of tyrosine kinases, such as Janus kinase 2 (JAK2), resulting in constitutive activation and various hematologic malignancies (42). JAK2 associates with and is activated by a complex of polycystin 1 and polycystin 2 in the JAK-STAT signaling pathway, mutations in which can result in deregulated cell proliferation and differentiation (43). SamCystin could also participate in renal morphogenesis as it has been shown that bifunctional apoptosis regulator protein mediates *in vitro* apoptosis through the interaction of its SAM domain with Bcl-2 (31).

One of the important features of SamCystin lies in that it is a novel protein that is structurally completely unrelated to the polycystins 1 and 2 as well as any other proteins associated with human cystic kidney disease. Recently, increasing evidence has been accumulated for the role of primary cilia in the pathogenesis of cyst formation as a result of the localization of Bicaudal C; cystin; fibrocystin; polaris; inversin; nephrocystins 1, 3, 4, and 5; polycystins 1 and 2; and kinesin-II 3a subunit (3,44,45) to this organelle. Therefore, an important development of our study will be to test whether the SamCystin protein is also part of the cilium despite its particular structure. In light of reports of cyst occurrence in other renal structures, including the collecting duct and distal nephron (46), further investigations into the biologic function of SamCystin and the effects of the mutation involved in the development of abnormal tubule architecture in the PKD rat may define new pathways and molecular mechanisms that contribute to renal cyst formation. Structural studies of SamCystin will help with resolving binding surfaces in SAM–domain interactions, identifying interacting proteins in the kidney, and characterizing the molecular

pathways involving SamCystin to uncover important hitherto unknown contributing factors in normal renal development and in cyst formation.

The identification of the mutation that is likely to cause renal cyst development in the PKD/Mhm(cy/+) rat in a novel gene encoding SamCystin provides new opportunities for further dissecting mechanisms that control cystogenesis and modulate PKD severity (11). Both this novel gene and genes that encode proteins that interact with SamCystin call for large-scale genetic and functional studies in human PKD that may have significant implications for the clinical classification of cystic kidney diseases and the development of novel therapeutic strategies.

## Acknowledgments

This work is supported by the Wellcome Trust and research grants from the National Kidney Research Fund (R27/2/99) and the European Commission (QLRT-2001-01104). The eukaryotic expression vector pEBG was provided by Tom Force. The cy rat strain of the American colony was obtained from Vicente Torres (Mayo Clinic, Rochester, MN). D.G. holds a Wellcome Senior Fellowship in Basic Biomedical Science (05773).

We are grateful for the expert technical assistance of Vera Könecke and Larissa Osten.

## References

- Igarashi P, Somlo S: Genetics and pathogenesis of polycystic kidney disease. *J Am Soc Nephrol* 13: 2384–2398, 2002
- Ariza M, Alvarez V, Marin R, Aguado S, Lopez-Larrea C, Alvarez J, Menendez MJ, Coto E: A family with a milder form of adult dominant not linked to the PKD1 (16p) or PKD2 (4q) genes. *J Med Genet* 34: 587–589, 1997
- Guay-Woodford LM: Murine models of polycystic kidney disease: Molecular and therapeutic insights. *Am J Physiol Renal Physiol* 285: F1034–F1049, 2003
- Schafer K, Gretz N, Bader M, Oberbaumer I, Eckardt KU, Kriz W, Bachmann S: Characterization of the Han:SPRD rat model for hereditary polycystic kidney disease. *Kidney Int* 46: 134–152, 1994
- Gretz N, Kranzlin B, Pey R, Schieren G, Bach J, Obermuller N, Ceccherini I, Kloting I, Rohmeiss P, Bachmann S, Hafner M: Rat models of autosomal dominant polycystic kidney disease. *Nephrol Dial Transplant* 11[Suppl 6]: 46–51, 1996
- Bihoreau MT, Ceccherini I, Browne J, Kranzlin B, Romeo G, Lathrop GM, James MR, Gretz N: Location of the first genetic locus, PKDr1, polycystic kidney disease in Han:SPRD cy/+ rat. *Hum Mol Genet* 6: 609–613, 1997
- Woo D, Shya S, Kurtz I: Localisation and genetic mapping of the polycystic kidney disease mutation in cy rat [Abstract]. *J Am Soc Nephrol* 7: A1797, 1996
- Nagao S, Ushijima T, Kasahara M, Yamaguchi T, Kusaka M, Matsuda J, Nagao M, Takahashi H: Closely linked polymorphic markers for determining the autosomal dominant allele (Cy) in rat polycystic kidney disease. *Biochem Genet* 37: 227–235, 1999
- Steen RG, Kwitek-Black AE, Glenn C, Gullings-Handley J, Van Etten W, Atkinson OS, Appel D, Twigger S, Muir M, Mull T, Granados M, Kissebah M, Russo K, Crane R, Popp M, Peden M, Matise T, Brown DM, Lu J, Kingsmore S, Tonellato PJ, Rozen S, Slonim D, Young P, Knoblauch M, Provoost A, Ganten D, Colman SD, Rothberg J, Lander ES, Jacob HJ: A high-density integrated genetic linkage and radiation hybrid map of the laboratory rat. *Genome Res* 9: AP1–AP8, 1999
- Wilder SP, Bihoreau MT, Argoud K, Watanabe TK, Lathrop M, Gauguier D: Integration of the rat recombination and EST maps in the rat genomic sequence and comparative mapping analysis with the mouse genome. *Genome Res* 14: 758–765, 2004
- Bihoreau MT, Megel N, Brown JH, Kranzlin B, Crombez L, Tychinskaya Y, Broxholme J, Kratz S, Bergmann V, Hoffman S, Gauguier D, Gretz N: Characterization of a major modifier locus for polycystic kidney disease (Modpkdr1) in the Han:SPRD(cy/+) rat in a region conserved with a mouse modifier locus for Alport syndrome. *Hum Mol Genet* 11: 2165–2173, 2002
- Watanabe TK, Bihoreau MT, McCarthy LC, Kiguwa SL, Hishigaki H, Tsuji A, Browne J, Yamasaki Y, Mizoguchi-Miyakita A, Oga K, Ono T, Okuno S, Kanemoto N, Takahashi E, Tomita K, Hayashi H, Adachi M, Webber C, Davis M, Kiel S, Knights C, Smith A, Critcher R, Miller J, Thangarajah T, Day PJ, Hudson JR Jr, Irie Y, Takagi T, Nakamura Y, Goodfellow PN, Lathrop GM, Tanigami A, James MR: A radiation hybrid map of the rat genome containing 5,255 markers. *Nat Genet* 22: 27–36, 1999
- Arnold C, Hodgson IJ: Vectorette PCR: A novel approach to genomic walking. *PCR Methods Appl* 1: 39–42, 1991
- Woon PY, Osogawa K, Kaisaki PJ, Zhao B, Catanese JJ, Gauguier D, Cox R, Levy ER, Lathrop GM, Monaco AP, de Jong PJ: Construction and characterization of a 10-fold genome equivalent rat P1-derived artificial chromosome library. *Genomics* 50: 306–316, 1998
- Obermuller N, Gretz N, Kriz W, Reilly RF, Witzgall R: The swelling-activated chloride channel CIC-2, the chloride channel CIC-3, and CIC-5, a chloride channel mutated in kidney stone disease, are expressed in distinct subpopulations of renal epithelial cells. *J Clin Invest* 101: 635–642, 1998
- Ausubel FA, Brent R, Kingston RE, Moore DD, Seidman JG, Smith JA, Struhl K: *Current Protocols in Molecular Biology*, New York, John Wiley & Sons, 1996
- Zor T, Selinger Z: Linearization of the Bradford protein assay increases its sensitivity: Theoretical and experimental studies. *Anal Biochem* 236: 302–308, 1996
- Bihoreau MT, Gauguier D, Kato N, Hyne G, Lindpaintner K, Rapp JP, James MR, Lathrop GM: A linkage map of the rat genome derived from three F2. *Genome Res* 7: 434–440, 1997
- Aparicio S, Chapman J, Stupka E, Putnam N, Chia JM, Dehal P, Christoffels A, Rash S, Hoon S, Smit A, Gelpke MD, Roach J, Oh T, Ho IY, Wong M, Detter C, Verhoef F, Predki P, Tay A, Lucas S, Richardson P, Smith SF, Clark MS, Edwards YJ, Doggett N, Zharkikh A, Tavtigian SV, Pruss D, Barnstead M, Evans C, Baden H, Powell J, Glusman G, Rowen L, Hood L, Tan YH, Elgar G, Hawkins T, Venkatesh B, Rokhsar D, Brenner S: Whole-genome shotgun assembly and analysis of the genome of *Fugu rubripes*. *Science* 297: 1301–1310, 2002
- Dehal P, Satou Y, Campbell RK, Chapman J, Degnan B, De Tomaso A, Davidson B, Di Gregorio A, Gelpke M, Goodstein DM, Harafuji N, Hastings KE, Ho I, Hotta K, Huang W, Kawashima T, Lemaire P, Martinez D, Meinertzhagen IA, Nacula S, Nonaka M, Putnam N, Rash S, Saiga H, Satake M, Terry A, Yamada L, Wang HG, Awazu S, Azumi K, Boore J, Branno M, Chin-Bow S, DeSantis R, Doyle S,

- Francino P, Keys DN, Haga S, Hayashi H, Hino K, Imai KS, Inaba K, Kano S, Kobayashi K, Kobayashi M, Lee BI, Makabe KW, Manohar C, Matassi G, Medina M, Mochizuki Y, Mount S, Morishita T, Miura S, Nakayama A, Nishizaka S, Nomoto H, Ohta F, Oishi K, Rigoutsos I, Sano M, Sasaki A, Sasakura Y, Shoguchi E, Shin-i T, Spagnuolo A, Stainier D, Suzuki MM, Tassy O, Takatori N, Tokuoka M, Yagi K, Yoshizaki F, Wada S, Zhang C, Hyatt PD, Larimer F, Detter C, Doggett N, Glavina T, Hawkins T, Richardson P, Lucas S, Kohara Y, Levine M, Satoh N, Rokhsar DS: The draft genome of *Ciona intestinalis*: Insights into chordate and vertebrate origins. *Science* 298: 2157–2167, 2002
21. Andrade MA, Perez-Iratxeta C, Ponting CP: Protein repeats: Structures, functions, and evolution. *J Struct Biol* 134: 117–131, 2001
  22. Kim CA, Bowie JU: SAM domains: Uniform structure, diversity of function. *Trends Biochem Sci* 28: 625–628, 2003
  23. Kyba M, Brock HW: The SAM domain of polyhomeotic, RAE28, and scm mediates specific interactions through conserved residues. *Dev Genet* 22: 74–84, 1998
  24. Serra-Pages C, Medley QG, Tang M, Hart A, Streuli M: Liprins, a family of LAR transmembrane protein-tyrosine phosphatase-interacting proteins. *J Biol Chem* 273: 15611–15620, 1998
  25. Stapleton D, Balan I, Pawson T, Sicheri F: The crystal structure of an Eph receptor SAM domain reveals a mechanism for modular dimerization. *Nat Struct Biol* 6: 44–49, 1999
  26. Green JB, Gardner CD, Wharton RP, Aggarwal AK: RNA recognition via the SAM domain of Smaug. *Mol Cell* 11: 1537–1548, 2003
  27. Schultz J, Ponting CP, Hofmann K, Bork P: SAM as a protein interaction domain involved in developmental regulation. *Protein Sci* 6: 249–253, 1997
  28. Tu H, Barr M, Dong DL, Wigler M: Multiple regulatory domains on the Byr2 protein kinase. *Mol Cell Biol* 17: 5876–5887, 1997
  29. Serra-Pages C, Kedersha NL, Fazikas L, Medley Q, Debant A, Streuli M: The LAR transmembrane protein tyrosine phosphatase and a coiled-coil LAR-interacting protein colocalize at focal adhesions. *EMBO J* 14: 2827–2838, 1995
  30. Kasten M, Giordano A: Cdk10, a Cdc2-related kinase, associates with the Ets2 transcription factor and modulates its transactivation activity. *Oncogene* 20: 1832–1838, 2001
  31. Zhang H, Xu Q, Krajewski S, Krajewska M, Xie Z, Fuess S, Kitada S, Pawlowski K, Godzik A, Reed JC: BAR: An apoptosis regulator at the intersection of caspases and Bcl-2 family proteins. *Proc Natl Acad Sci U S A* 97: 2597–2602, 2000
  32. Seidel JJ, Graves BJ: An ERK2 docking site in the Pointed domain distinguishes a subset of ETS transcription factors. *Genes Dev* 16: 127–137, 2002
  33. Weil D, El-Amraoui A, Masmoudi S, Mustapha M, Kikkawa Y, Laine S, Delmaghani S, Adato A, Nadifi S, Zina ZB, Hamel C, Gal A, Ayadi H, Yonekawa H, Petit C: Usher syndrome type I G (USH1G) is caused by mutations in the gene encoding SANS, a protein that associates with the USH1C protein, harmonin. *Hum Mol Genet* 12: 463–471, 2003
  34. Sheng M, Kim E: The Shank family of scaffold proteins. *J Cell Sci* 113: 1851–1856, 2000
  35. Tabuchi K, Biederer T, Butz S, Sudhof TC: CASK participates in alternative tripartite complexes in which Mint 1 competes for binding with caskin 1, a novel CASK-binding protein. *J Neurosci* 22: 4264–4273, 2002
  36. Lyons RJ, Deane R, Lynch DK, Ye ZS, Sanderson GM, Eyre HJ, Sutherland GR, Daly RJ: Identification of a novel human tankyrase through its interaction with the adaptor protein Grb14. *J Biol Chem* 276: 17172–17180, 2001
  37. Yan W, Rajkovic A, Viveiros MM, Burns KH, Eppig JJ, Matzuk MM: Identification of Gasz, an evolutionarily conserved gene expressed exclusively in germ cells and encoding a protein with four ankyrin repeats, a sterile-alpha motif, and a basic leucine zipper. *Mol Endocrinol* 16: 1168–1184, 2002
  38. Cogswell C, Price SJ, Hou X, Guay-Woodford LM, Flaherty L, Bryda EC: Positional cloning of jcpk/bpk locus of the mouse. *Mamm Genome* 14: 242–249, 2003
  39. Saffman EE, Styhler S, Rother K, Li W, Richard S, Lasko P: Premature translation of oskar in oocytes lacking the RNA-binding protein bicaudal-C. *Mol Cell Biol* 18: 4855–4862, 1998
  40. Kikkawa Y, Shitara H, Wakana S, Kohara Y, Takada T, Okamoto M, Taya C, Kamiya K, Yoshikawa Y, Tokano H, Kitamura K, Shimizu K, Wakabayashi Y, Shiroishi T, Kominami R, Yonekawa H: Mutations in a new scaffold protein Sans cause deafness in Jackson shaker mice. *Hum Mol Genet* 12: 453–461, 2003
  41. Yoder BK, Hou X, Guay-Woodford LM: The polycystic kidney disease proteins, polycystin-1, polycystin-2, polaris, and cystin, are co-localized in renal cilia. *J Am Soc Nephrol* 13: 2508–2516, 2002
  42. Kim CA, Phillips ML, Kim W, Gingery M, Tran HH, Robinson MA, Faham S, Bowie JU: Polymerization of the SAM domain of TEL in leukemogenesis and transcriptional repression. *EMBO J* 20: 4173–4182, 2001
  43. Bhunia AK, Piontek K, Boletta A, Liu L, Qian F, Xu PN, Germino FJ, Germino GG: PKD1 induces p21(waf1) and regulation of the cell cycle via direct activation of the JAK-STAT signaling pathway in a process requiring PKD2. *Cell* 109: 157–168, 2002
  44. Olbrich H, Fliegauf M, Hoefele J, Kispert A, Otto E, Volz A, Wolf MT, Sasmaz G, Trauer U, Reinhardt R, Sudbrak R, Antignac C, Gretz N, Walz G, Schermer B, Benzing T, Hildebrandt F, Omran H: Mutations in a novel gene, NPHP3, cause adolescent nephronophthisis, tapeto-retinal degeneration and hepatic fibrosis. *Nat Genet* 34: 455–459, 2003
  45. Nauli SM, Zhou J: Polycystins and mechanosensation in renal and nodal cilia. *Bioessays* 26: 844–856, 2004
  46. Wu G, D'Agati V, Cai Y, Markowitz G, Park JH, Reynolds DM, Maeda Y, Le TC, Hou H Jr, Kucherlapati R, Edelmann W, Somlo S: Somatic inactivation of Pkd2 results in polycystic kidney disease. *Cell* 93: 177–188, 1998
  47. Goodstadt L, Ponting CP: CHROMA: Consensus-based colouring of multiple alignments for publication. *Bioinformatics* 17: 845–846, 2001
  48. Russell RB, Barton GJ: Multiple protein sequence alignment from tertiary structure comparison: Assignment of global and residue confidence levels. *Proteins* 14: 309–323, 1992